Available online at www.sciencedirect.com
ScienceDirect
Optical Materials 30 (2007) 346–350
OPTICAL Materials
www.elsevier.com/locate/optmat

Optical and morphological properties of MBE grown wurtzite $Cd_xZn_{1-x}O$ thin films

J.W. Mares [a], F.R. Ruhge [a], A.V. Thompson [a], P.G. Kik [a], A. Osinsky [b], B. Hertog [b], A.M. Dabiran [b], P.P. Chow [b], W.V. Schoenfeld [a,*]

[a] *CREOL: College of Optics and Photonics, University of Central Florida, 4000 Central Florida Blvd., Orlando, FL 32816-2700, United States*
[b] *SVT Associates, Eden Prairie, MN, United States*

Received 6 July 2006; received in revised form 7 November 2006; accepted 20 November 2006
Available online 24 January 2007

Abstract

Wurtzite $Cd_xZn_{1-x}O$ epilayers with cadmium concentrations ranging from $x = 0.02$ to 0.30 were investigated using photoluminescence, transmission/reflection spectroscopy, and atomic force microscopy. The $Cd_xZn_{1-x}O$ photoluminescence peak was found to shift through the visible region from 421 (2.95 eV) to 619 nm (2.0 eV) as the cadmium concentration was increased from 2% to 30%. An additional broad photoluminescence peak was observed and is attributed to deep levels – the center of the broad peak was found to shift from 675 to 750 nm as the cadmium concentration was increased. RMS roughness of the epilayers increased from 1.5 nm ($x = 0.02$) to 9.2 nm ($x = 0.30$), as determined from atomic force microscopy. The demonstrated visible wavelength tunability throughout the visible range verifies the viability of using wurtzite $Cd_xZn_{1-x}O$ compounds for visible light emission in future optoelectronic devices.

PACS: 78.55; 42.25.B; 81.15.H; 61.16.C

Keywords: Zinc oxide; Cadmium zinc oxide; Wide band gap; Wurtzite oxides

1. Introduction

The use of ZnO-based compounds in optoelectronic devices has advanced substantially in recent years [1–6]. As a wide band gap semiconductor ($E_{g,RT} = 3.37$ eV), ZnO is a suitable material for ultraviolet light emitting devices. Much of the current interest in wurtzite ZnO is a result of its strikingly similar properties to the much more mature wurtzite GaN system used in commercially available LEDs and other electronic devices. This interest has been further strengthened by several potential advantages of ZnO over GaN. First, ZnO substrates have become commercially available with relatively low dislocation densities of 10^4–10^5 cm^{-2} [7], enabling homoepitaxial growth that may result in a considerable reduction of interface dislocations. Additionally, high quality ZnO epilayers can be grown on Al_2O_3 substrates, mediated by low temperature MgO buffer layers, allowing one to avoid the relatively larger expense of ZnO substrates. Perhaps one of the more attractive properties of ZnO is its compatibility with wet etch chemistries – its GaN counterpart is generally limited to dry etching methods with low selectivities between the epilayer and photoresist mask [8]. In fact, selective wet etching has recently been demonstrated for the ZnO/$Cd_xZn_{1-x}O$ system [9]. This should enable inexpensive device processing and engender new optical structures and devices based on ZnO ternary heterostructures. Lastly, the exceptional exciton binding energy of ZnO (60 meV) enables efficient photoluminescence at room temperature and has allowed researchers to realize high temperature UV lasing with epitaxially grown ZnO films [10–12].

* Corresponding author. Tel.: +1 407 823 6898; fax: +1 407 823 6880.
E-mail address: winston@creol.ucf.edu (W.V. Schoenfeld).

0925-3467/$ - see front matter © 2006 Elsevier B.V. All rights reserved.
doi:10.1016/j.optmat.2006.11.058

While bulk ZnO itself offers many potential benefits, advanced heterostructures require the ability to tune the bang gap and confinement energies of the individual layers. This has recently been achieved through alloying with cadmium or magnesium, shifting the band gap to longer or shorter wavelengths, respectively [5,13–15]. Despite issues with solid solubility [16], incorporation of Mg and Cd has improved dramatically using techniques such as pulsed laser deposition (PLD), laser assisted molecular beam epitaxy (LMBE) and, in particular, remote plasma enhanced metalorganic chemical vapor deposition (RPE-MOCVD). Current data holds that the band gap energy of wurtzite ternary ZnO compounds can successfully be tuned from ~1.7 eV to 4 eV by appropriate Cd or Mg integration [5,6,17].

In order to effectively engineer sophisticated heterostructure devices, ternary $Cd_xZn_{1-x}O$ and $Mg_xZn_{1-x}O$ alloys must be well characterized in terms of optical properties as well as surface quality. In this study, $Cd_xZn_{1-x}O$ thin films were investigated as candidates for achieving optical devices in the UV and visible range. Epilayers of various Cd concentrations were grown by RF plasma-assisted molecular beam epitaxy and characterized using spectrophotometry, power-dependent photoluminescence, and atomic force microscopy.

2. Method

$Cd_xZn_{1-x}O$ epitaxial films were grown by RF plasma-assisted molecular beam epitaxy (MBE) in a SVT Associates growth chamber, as reported elsewhere [1]. Growth was carried out on GaN-buffered, *c*-plane sapphire templates. The GaN epitaxial layer (less than 1 μm in thickness) assists in nucleation of a subsequent ZnO buffer layer, 100–200 nm in thickness. $Cd_xZn_{1-x}O$ epilayers of varying Cd concentration were then grown to a thickness of 200 nm at temperatures below 600 °C using 6 N purity Zn and Cd elemental sources. The resultant wurtzite $Cd_xZn_{1-x}O$ epilayers were investigated by X-ray diffraction, and the Cd composition in each sample was determined by Rutherford backscattering (RBS) and secondary ion mass spectroscopy (SIMS) [1].

Photoluminescence (PL) measurements were carried out using a Spectra Physics BeamLok 2060 krypton ion (Kr^+) gas laser as the pump source, tuned to 350.7 nm (3.535 eV). The output power ranged from 120 to 140 mW, as measured on a Newport 818 optical power meter. The optical power at the sample surface was varied with OD filters from 0.08 mW to 33 mW. The beam was focused with standard optical elements to a spot size of ~1 mm, providing intensities ranging from 0.01 to 4.2 W/cm^2 at the surface of the epitaxial layers. PL from the epilayers was collected with high numerical aperture lens and directed into an Acton 2300i Monochromator and detected using a thermoelectrically cooled Andor CCD array. All PL spectra were corrected to compensate for system response. PL measurements were taken from $Cd_xZn_{1-x}O$ samples ranging in Cd concentration from $x = 0.02$ to $x = 0.30$. Spectrophotometry in the 190–1300 nm range was done using a Cary500 Varian spectrophotometer. Absorption characteristics of the epilayers were determined from reflection and transmission measurements. In order to reduce multiple reflection artifacts in the absorption curves, reflection measurements were first made on the thin films using a single-bounce technique at an incident angle of 24°. Subsequent transmission measurements were made at the same angle, and from these measurements absorption was extracted. Lastly, roughness measurements and surface profiles were conducted using a Veeco Dimension 3100 atomic force microscope (AFM) in tapping mode.

3. Results and discussion

The measured absorption and PL spectra for the $Cd_xZn_{1-x}O$ epilayers as a function of Cd concentration are given in Fig. 1. Prior to measurement, the Cd concentration in each epilayer was determined using RBS and SIMS. As the Cd concentration is increased from 2% to 30%, a systematic shift in the PL peak from the $Cd_xZn_{1-x}O$ epilayers is observed, moving from 421 nm (2.95 eV) to 619 nm (2.0 eV). The peaks are generally Gaussian-like in shape, though interference from multiple internal reflections has a modulating effect on the intensity. The magnitude of the PL for the various samples did not exhibit a clear dependence upon the cadmium concentration, however further investigations are planned to better understand the relation between PL position and magnitude on cadmium concentration. Determination of the PL peak position for the 30% $Cd_xZn_{1-x}O$ sample required peak fitting to separate the excitonic emission from the red defect band PL (discussed later). We anticipate a ±25 nm error associ-

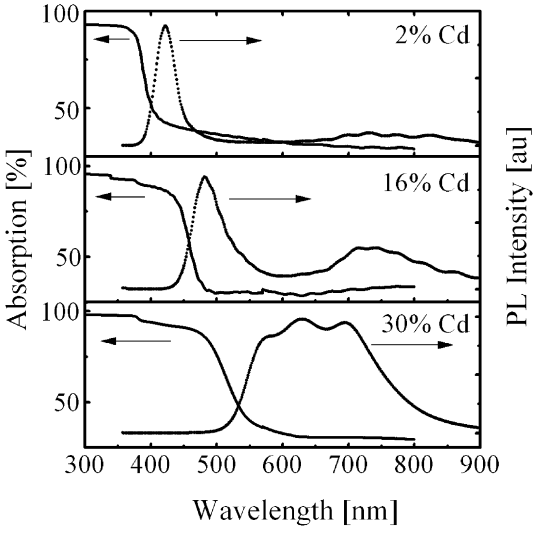

Fig. 1. Room temperature absorption and photoluminescence spectra from $Cd_xZn_{1-x}O$ epilayers with $x = 0.02$, 0.16, and 0.30. A systematic shift of the absorption edge and photoluminescence peak is observed with increasing Cd concentration.

ated with the Gaussian fit for this sample, corresponding to a PL peak energy error of roughly ±80 meV. The locations of the PL peaks are in good agreement with published values for $Cd_xZn_{1-x}O$ grown by other techniques [5,6]. Absorption data correlates well with the PL spectra, also showing a systematic shift to longer wavelengths for increasing Cd concentrations. Small features attributed to the buffer layers are present in the spectra near the 365–368 nm absorption edges of the ZnO and GaN. A summary of the PL peak energy and corresponding full-width half maximum (FWHM) from all $Cd_xZn_{1-x}O$ epilayers is given in Fig. 2. The PL energies correspond to wavelengths that cover the complete range of visible wavelengths up to 620 nm. The dependence of the PL energy on Cd concentration was determined through a non-linear curve fit, and is given approximately by $E_{PL}(x_{Cd}) = 3.37 - 0.077x_{Cd} + 0.0011x_{Cd}^2$ eV. The FWHM of the peaks increases from 36 to 144 nm as the peak center shifts towards longer wavelengths for increased Cd concentration up to 30%. A corresponding reduction in the abruptness of the absorption spectra (see Fig. 1) is also observed. We attribute this to a greater amount of compositional variations in the epilayers. This is supported by the XRD data from these samples reported elsewhere [1] that demonstrates a greater FWHM as the Cd concentration is increased. It is important to note that while the FWHM increases, the wurtzite structure of the epilayers is maintained given that no cubic phase peaks are present in the XRD data.

A broad PL peak centered between 675 nm and 750 nm is observed in each of the PL spectra. Similar emission has been observed in bulk ZnO [12], however the emission is generally found at shorter wavelengths around 565 nm. GaN has a yellow emission line which is attributed to deep level donor/acceptor states [18–20], and similar luminescence has been observed from $Cd_xZn_{1-x}O$ grown on Silicon substrates [17]. To further characterize the red luminescence, power-dependent PL (PDPL) data was taken. Fig. 3 provides a log scale plot of the integrated

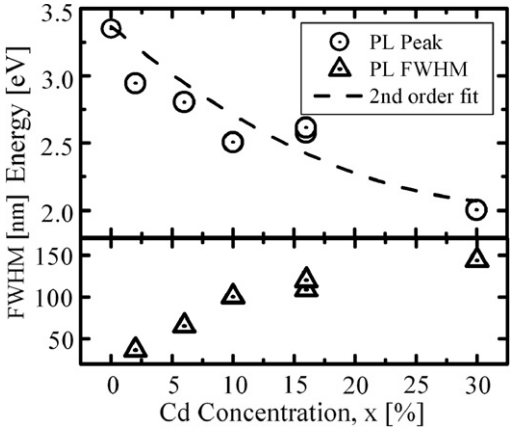

Fig. 2. Photoluminescence peak energy (top) and FWHM (bottom) as a function of cadmium concentration in the $Cd_xZn_{1-x}O$ epilayers.

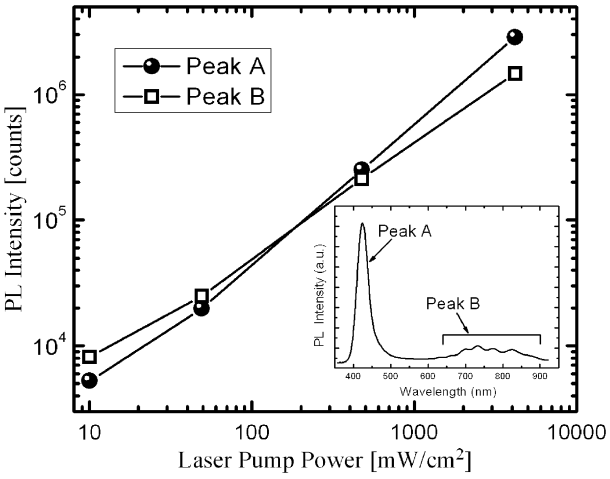

Fig. 3. Integrated intensity of band edge (Peak A) and red band (Peak B) photoluminescence as a function of laser pump power for a $Cd_{0.02}Zn_{0.98}O$ epilayer. Inset provides peak definition used for figure.

intensities of the PL peaks as a function of laser pump power. As indicated in the inset in the figure, Peak A corresponds to the band edge luminescence from the $Cd_xZn_{1-x}O$ epilayer and Peak B is assigned to the red band luminescence. Under low excitation powers, the red band luminescence (Peak B) is found to have a greater integrated intensity than that of the band edge luminescence (Peak A). As pump power is increased the band edge luminescence begins to dominate over the red band luminescence. Specifically, for a pump laser irradiance of 10 mW/cm^2 the red band comprises 61% of the total integrated PL. As the pump laser irradiance is increased to 4.2 W/cm^2 the contribution of the red band decreased to less than 28% of the total integrated PL. Others have observed saturation of deep levels in PDPL spectra [21,22], however we did not reach the saturation level of the red band in our samples due to lack of additional pump laser power. We assign the red band luminescence observed to deep levels in the $Cd_xZn_{1-x}O$ epilayers, however additional work is needed to further assign the luminescence to specific levels.

The surface morphology of the $Cd_xZn_{1-x}O$ epilayers was investigated using AFM in tapping mode (TMAFM). TMAFM images are presented in Fig. 4a–d with a RMS roughness summary from all samples provided in Fig. 4e. For comparison, Fig. 4a shows the TMAFM image from a GaN template used for the $Cd_xZn_{1-x}O$ epitaxial growth. The GaN layer is found to be of good quality, with a RMS roughness of 1.5 nm. The surface of the $Cd_{0.02}Zn_{0.98}O$ epilayer has a RMS roughness of only 2.8 nm, and is highly uniform (Fig. 4b). A moderate density ($\sim 10^8$ cm^{-2}) of surface features with a base width of 200 nm and a height of 10–20 nm occur sporadically on the surface. As the Cd concentration in the $Cd_xZn_{1-x}O$ epilayers is increased to 10% and 30%, the RMS roughness increases to 4.2 nm and 9.2 nm, respectively. For increasing concentrations of Cd, the density of surface features increases as does their respective aspect ratios. Interestingly, the roughness

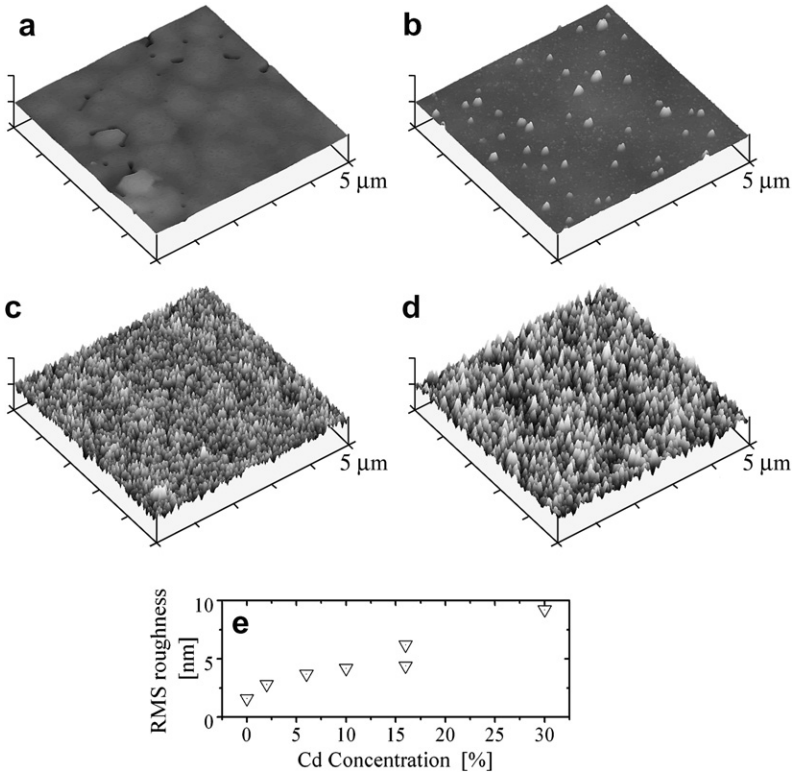

Fig. 4. Tapping mode atomic force microscope images of the epilayer surface for the GaN buffer layer on Al_2O_3 (a) and $Cd_xZn_{1-x}O$ with $x = 0.02$, 0.10, and 0.30 (b–d). A summary of the RMS roughness values from the epilayers is given in (e).

increase is found to be approximately linear as a function of Cd concentration.

4. Conclusions

Wurtzite $Cd_xZn_{1-x}O$ epilayers were produced by plasma-assisted MBE on GaN-buffered Al_2O_3 substrates. Samples with Cd concentrations ranging from $x = 0.02$ to $x = 0.30$ were examined for optical and morphological quality. The $Cd_xZn_{1-x}O$ films exhibited visible photoluminescence that shifted throughout the complete visible range with increasing cadmium content up to 30%. An additional saturable emission peak was observed in the red region of the spectra for all samples, with peaks between 740 and 775 nm and is associated with deep donor and acceptor levels. A strict dependence of PL efficiency on cadmium concentration was not observed. Transmission and reflection measurements were used to generate the absorption curves for the $Cd_xZn_{1-x}O$ epilayers as a function of Cd concentration. The absorption data was in good agreement with the PL spectra, verifying the potential use of $Cd_xZn_{1-x}O$ compounds for visible light emitting devices. AFM measurements revealed good quality films for lower concentration samples ($x < 0.16$), with roughness increasing linearly with increasing cadmium content up to $x = 0.30$. These results demonstrate that alloying of Cd with ZnO is a viable approach to creating visible wavelength optical devices and is suitable for advanced compound heterostructures for high-efficiency emission.

Acknowledgement

The authors would like to acknowledge the support of this research through funding provided by the Army Research Office (Contract# W911NF-05-C-0024), monitored by Dr. Michael Gerhold.

References

[1] A. Osinsky, J.W. Dong, J.Q. Xie, B. Hertog, A.M. Dabiran, P.P. Chow, S.J. Pearton, D.P. Norton, D.C. Look, W. Schoenfeld, O. Lopatiuk, L. Chernyak, M. Cheung, A.N. Cartwright, M. Gerhold, Mater. Res. Soc. Symp. Proc. 892 (2006).
[2] C. Morhain, X. Tang, M. Teisseire-Doninelli, B. Lo, M. Laügt, J.M. Chauveau, B. Vinter, O. Tottereau, P. Vennéguès, C. Deparis, G. Neu, Superlattices Microstruct. 30 (2005) 455.
[3] Th. Gruber, C. Kirchner, R. Kling, F. Reuss, A. Waag, Appl. Phys. Lett. 84 (2004) 5359.
[4] J.J. Chen, F. Ren, Y. Li, D.P. Norton, S.J. Pearton, A. Osinsky, J.W. Dong, P.P. Chow, J.F. Weaver, Appl. Phys. Lett. 87 (2005) 192106.
[5] S. Shigemori, A. Nakamura, J. Ishihara, T. Aoki, J. Temmyo, Jpn. J. Appl. Phys. 43 (2004) L1088.
[6] A. Nakamura, J. Ishihara, S. Shigemori, K. Yamamoto, T. Aoki, H. Gotoh, J. Temmyo, Jpn. J. Appl. Phys. 43 (2004) L1452.
[7] D.C. Look, Mater. Sci. Eng. B 80 (2001) 383.
[8] Z.-Q. Fang, D.C. Look, X.-L. Wang, J. Han, F.A. Khan, I. Adesida, Appl. Phys. Lett. 82 (2003) 1562.

[9] J.J. Chen, F. Ren, D.P. Norton, S.J. Pearton, A. Osinsky, J.W. Dong, S.N.G. Chu, Electrochem. Solid-State Lett. 8 (2005) G359.
[10] D.C. Reynolds, D.C. Look, B. Jogai, Solid State Commun. 99 (1996) 873.
[11] D.M. Bagnall, Y.F. Chen, Z. Zhu, T. Yao, S. Koyama, M.Y. Shen, T. Goto, Appl. Phys. Lett. 70 (1997) 2230.
[12] H.D. Li, S.F. Yu, S.P. Lau, E.S.P. Leong, H.Y. Yang, T.P. Chen, A.P. Abiyasa, C.Y. Ng, Adv. Mater. 18 (2006) 771.
[13] A. Ohtomo, M. Kawasaki, T. Koida, K. Masubuchi, H. Koinuma, Y. Sakurai, Y. Yoshida, T. Yasuda, Y. Segawa, Appl. Phys. Lett. 72 (1998) 2466.
[14] T. Makino, Y. Segawa, M. Kawasaki, A. Ohtomo, R. Shiroki, K. Tamura, T. Yasuda, H. Koinuma, Appl. Phys. Lett. 78 (2001) 1237.
[15] L.M. Kukreja, S. Barik, P. Misra, J. Cryst. Growth 268 (2004) 531.
[16] J.F. Sarver, F.L. Katnack, F.A. Hummel, J. Electrochem. Soc. 106 (1959) 960.
[17] N.B. Chen, C.H. Sui, Mater. Sci. Eng. B 126 (2006) 16.
[18] S.K. Hong, H.J. Ko, Y. Chen, T. Hanada, T. Yao, J. Vac. Sci. Technol. B 18 (2000) 2313.
[19] Z. Ye, D. Ma, J. He, J. Huang, B. Zhao, X. Luo, Z. Xu, J. Cryst. Growth 256 (2003) 78.
[20] G.-C. Yi, B.W. Wessels, Appl. Phys. Lett. 69 (1996) 3028.
[21] I. Shalish, L. Kronik, G. Segal, Y. Rosenwaks, Y. Shapira, Phys. Rev. B 59 (1999) 9748.
[22] W. Grieshaber, E.F. Schubert, I.D. Goepfert, R.F. Karlicek, M.J. Schurman, C. Tran, J. Appl. Phys. 80 (1996) 4615.